THE JOURNAL OF
PHYSICAL CHEMISTRY A

Article

pubs.acs.org/JPCA

Structural Evolution and Electronic Properties of $V_nC_2^{0/-}$ and $V_nC_4^{0/-}$ (n = 1−6) Clusters: Insights from Photoelectron Spectroscopy and Theoretical Calculations

Jinyun Yuan,[†,§] Peng Wang,[‡] Gao-Lei Hou,[‡] Gang Feng,[‡] Wen-Jing Zhang,[‡] Xi-Ling Xu,[‡] Hong-Guang Xu,[‡] Jinlong Yang,[*,†,∥] and Wei-Jun Zheng[*,‡]

[†]Hefei National Lab for Physical Sciences at Microscale, Department of Chemical Physics and [∥]Synergetic Innovation Center of Quantum Information and Quantum Physics, University of Science and Technology of China, Hefei, Anhui 230026, China

[‡]Beijing National Laboratory for Molecular Sciences, State Key Laboratory of Molecular Reaction Dynamics, Institute of Chemistry, Chinese Academy of Sciences, Beijing 100190, China

[§]Institute of Nanostructured Functional Materials, Huanghe Science and Technology College, Zhengzhou, Henan 450006, China

Supporting Information

ABSTRACT: The structural evolution and electronic properties of $V_nC_2^{-/0}$ and $V_nC_4^{-/0}$ (n = 1−6) clusters were investigated using photoelectron spectroscopy and density functional theory calculations. The adiabatic and vertical detachment energies of $V_nC_2^-$ and $V_nC_4^-$ (n = 1−6) clusters were obtained from their photoelectron spectra. The most stable structures were identified by comparing the results of our calculations with the experimental data. We found that the carbon atoms of $V_nC_2^{-/0}$ and $V_nC_4^{-/0}$ (n = 1−6) clusters were separated gradually with increasing number of vanadium atoms. For $V_nC_2^{-/0}$ (n = 3−6) and $V_nC_4^{-/0}$ (n = 4−6) clusters, the carbon atoms are separated by the vanadium atoms. The geometry of V_4C_4 is a cubic structure and the geometries of V_5C_4 and V_6C_4 are formed by one and two vanadium atoms capping the cubic V_4C_4 structure, respectively.

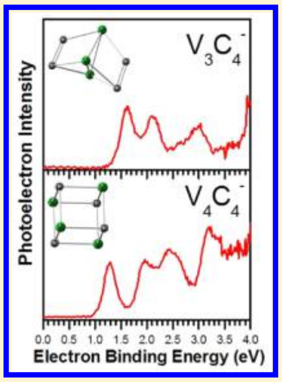

1. INTRODUCTION

Transition metal carbides possess unique physical and chemical properties, such as energy storage, higher electrical conductivity, high thermal conductivity, high melting point and hardness, as well as their excellent noble-metal-like catalytic activities.[1−3] In view of these unique properties, transition metal carbides have attracted increasing attention for potential applications. A few decades ago, it was found that some early transition metal carbides exhibited catalytic behavior similar to those of Pt-based catalysts in surface catalysis.[1] Recently, early transition metal carbides were found to be promising anode materials for Li-ion batteries.[2,3] The interaction of early transition metals with carbon has been found to form metallocarbohedrenes (Met-Cars) with M_8C_{12} stoichiometry.[4−6] They can also form two-dimensional transition metal carbide nanocrystals, whose structures and properties are similar to those of graphene.[7,8] It was recently reported that this type of early transition metal carbide can facilitate the catalytic growth of single- to few-layer graphene.[9] Regarding late transition metals, they are catalysts for carbon nanotube formation.[10] On the other hand, networked metallofullerenes can be formed by transition metals incorporated into carbon cages.[11]

Regarding vanadium carbide clusters, not only has Met-Car V_8C_{12} been found,[12] but also a cubic nanocrystal $V_{14}C_{13}$ cluster via laser vaporization of a metal sample with expansion gas seeded with methane or acetylene.[13] Helden et al. investigated vanadium-carbide nanocrystals using resonance-enhanced absorption of multiple infrared photons and found that the vanadium-carbide species produced are cubic and truncated nanocrystals with carbon vacancies at the corners.[14] Vanadium carbides have been found to have good oxygen reduction reaction catalytic activities.[15] Recently, V_2C monolayers (the two-dimensional material) have been predicted to be a promising anode material for Li-ion batteries.[16] Redondo et al. studied $VC_n^{0/\pm}$ (n = 2−8) clusters using density functional theory (DFT) calculations[17,18] and found a clear even−odd alternation in the stability of the fan-like structures of $VC_n^{0/+}$ (n = 2−8). The electronic states of the ground state $VC_2^{0/\pm}$ structures are predicted to be $^4B_1$, $^3B_1$, and $^5B_1$ at the DFT/B3LYP and CASSCF/MRSDCI levels.[19] Studies of $V_2C_2^-$ using photoelectron spectroscopy and DFT have indicated that the ground state structure has a planar distorted four-membered ring geometry with a transannular V−C bonding.[20] The electronic and geometric structures of $V_2C_n^-$ (n = 2−4) have been studied using photoelectron spectroscopy and DFT

Received: January 9, 2016
Revised: February 7, 2016
Published: February 12, 2016

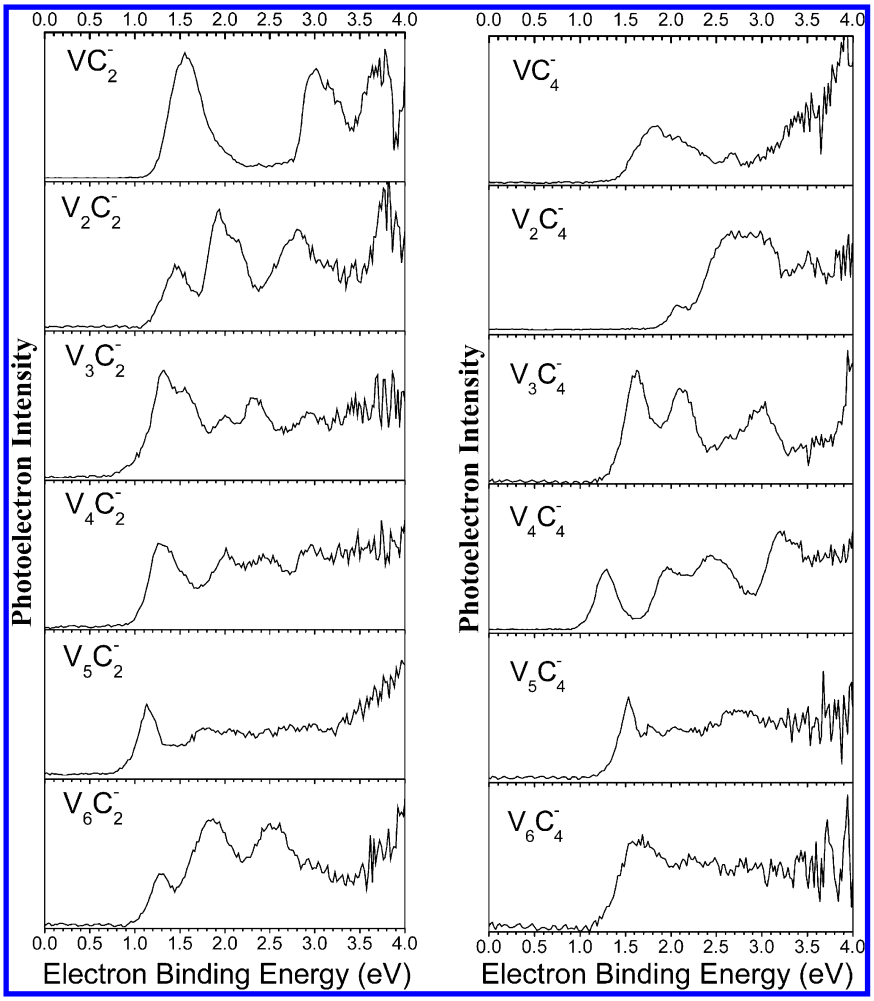

Figure 1. Photoelectron spectra of $V_nC_2^-$ and $V_nC_4^-$ (n = 1−6) cluster anions measured with 266 nm photons.

calculations.[21] Collision-induced dissociation of Met-Car $V_8C_{12}^+$ shows that it has multiple bonded metal atoms and contains C_2 units.[22] Castleman's group studied vanadium carbide clusters using time-of-flight mass spectroscopy. They found that the metal−carbon ratio has a substantial influence on the cluster products.[23] Although many vanadium carbides have been studied, the investigated cluster sizes are restricted to the small ones and some of the experimental spectra in the literature are of very low resolution. Thus, the information about the structural evolution of vanadium carbide clusters is limited, especially for cluster sizes beyond V_2C_4. The geometric and electronic structures are significant for understanding the physical and chemical properties of materials. In this study, we investigate the geometric and electronic structures of $V_nC_2^{-/0}$ and $V_nC_4^{-/0}$ (n = 1−6) clusters using photoelectron spectroscopy and DFT calculations. This may provide insight into the physical and chemical properties of these clusters and the growth mechanisms of vanadium carbide nanomaterials. Moreover, it could give some clues why the early transition metals can be used as catalysts of graphene growth and why the early transition metals can form the two-dimensional materials, also known as MXenes.

2. EXPERIMENTAL AND COMPUTATIONAL METHODS

2.1. Experimental Methods. The experiments were conducted on a home-built apparatus consisting of a time-of-flight mass spectrometer and a magnetic-bottle photoelectron spectrometer, which has been described elsewhere.[24] The anionic $V_nC_2^-$ and $V_nC_4^-$ (n = 1−6) clusters were generated in a laser vaporization source in which a rotating and translating vanadium−carbon target (mole ratio, V/C = 10/1) was ablated with the second harmonic light (532 nm) of a Nd:YAG laser (Continuum Surelite II−10) while helium gas with ∼4 atm backing pressure was allowed to expand through a pulsed valve over the vanadium−carbon target. The anionic $V_nC_2^-$ and $V_nC_4^-$ (n = 1−6) clusters were mass-selected and decelerated before being photodetached using the fourth (266 nm) harmonic light of a second Nd:YAG laser. The photodetached electrons were energy-analyzed by the magnetic-bottle photoelectron spectrometer. The photoelectron spectra were calibrated using the spectra of Cu^- and I^- taken under similar conditions. The energy resolution of the photoelectron spectrometer was approximately 40 meV for electrons with 1 eV kinetic energy.

2.2. Computational Methods. DFT with Becke's exchange[25] and the Perdew−Wang correlation functional (BPW91)[26] in the Gaussian 09 program[27] was used for all of the calculations in this work. The BPW91 functional has been widely applied to study transition-metal-containing systems.[28,29] We also used the BPW91 functional in our previous studies on $Co_nC_2^{0/-}$[30] and $CuV_n^{0/+}$[31,32] (n = 1−5) systems. Different functionals and basis sets were tested to confirm the reliability of the BPW91 functional and 6-311+G(d) basis set for $V_nC_2^{0/-}$ and $V_nC_4^{0/-}$ (n = 1−6) cluster systems (Table S1, Supporting Information). Thus, all of the calculations were carried out using the BPW91 exchange−correlation functional and the all-electron 6-311+G(d) basis set.

To search for the most stable structures of the $V_nC_2^{-/0}$ and $V_nC_4^{-/0}$ (n = 1−6) clusters, various initial structures with different spin multiplicities were taken into consideration. For example, we considered V_nC_4 (n = 1−6) clusters as vanadium clusters or several V atoms interacting with a C_4 chain, a C_4 ring, two carbon dimers, C_3 + C, and four C atoms. All possible spin multiplicities were considered until energy minimum structures were obtained, starting with a spin singlet state for the even-electron clusters (including spin multiplicities of 1, 3, 5, and 7) and a spin doublet state for the odd-electron clusters (including spin multiplicities of 2, 4, 6, and 8). Spin restricted and unrestricted calculations were carried out to find global minima of these clusters. Geometry optimizations were conducted without any symmetry constraints. The harmonic vibrational frequencies were calculated to ensure that the optimized structures correspond to real local minima. Natural population analysis (NPA) was performed with the natural bond orbital (NBO) program (version 3.1).[33] The zero-point vibrational energies were included for the adiabatic detachment energies (ADEs) and binding energies. Spin contamination was considered for all of the stable isomers to ensure that it was negligible.

The vertical detachment energies (VDEs) were calculated as the energy differences between the neutral and anionic species both with the geometries of the anionic species. The ADEs of the clusters were calculated based on the energy differences between neutral and anionic clusters, in which the neutral clusters were relaxed to the nearest local minima using the geometries of the anionic clusters as initial structures. For the anionic clusters with multiplicity M, the neutral species with multiplicities $M - 1$ and $M + 1$ were considered, and the lower energy spin multiplicity was used in the VDE and ADE calculations.

3. EXPERIMENTAL RESULTS

The photoelectron spectra of $V_nC_2^-$ and $V_nC_4^-$ (n = 1−6) clusters measured with 266 nm photons are shown in Figure 1. The VDEs and ADEs of these clusters obtained from the photoelectron spectra are listed in Tables 1 and 2. The ADEs were determined by drawing a straight line along the leading edge of the first peaks to cross the spectrum baselines and adding the instrumental resolution to the electron binding energy (EBE) values at the crossing points. The VDEs were obtained by measuring the maximum value of the first peak in the photoelectron spectra.

Photoelectron Spectra of $V_nC_2^-$ (n = 1−6). The 266 nm photoelectron spectrum of VC_2^- has three major features centered at 1.56, 3.01, and 3.72 eV. It also has a band feature above 3.9 eV. The features of the spectrum are consistent with those of the 532 and 355 nm spectra of VC_2^- reported by Li et al.[34] The spectrum of $V_2C_2^-$ at 266 nm shows four major peaks centered at 1.47, 1.94, 2.80, and 3.80 eV, and a shoulder peak at 2.09 eV. The 266 nm spectrum of $V_2C_2^-$ measured in this work is in agreement with the 355 nm spectrum reported by Tono et al.[20] For the $V_3C_2^-$ cluster, the 266 nm spectrum has a strong peak at 1.32 eV, three relatively weak peaks at 2.00, 2.33, and 2.93 eV, and a shoulder peak at 1.56 eV. The 266 nm spectrum of $V_4C_2^-$ exhibits at least four peaks centered at 1.28, 2.01, 2.42, and 2.97 eV. With respect to $V_5C_2^-$, the 266 nm spectrum has a peak centered at 1.14 eV, followed by a very broad peak in the range of 1.60−3.20 eV. There are three peaks centered at 1.29, 1.87, and 2.55 eV in the 266 nm spectrum of $V_6C_2^-$.

Table 1. Calculated Relative Energies (REs), VDEs, and ADEs (eV) of the Low-Energy Structures of $V_nC_2^-$ (n = 1−6) Clusters as Well as Their ADEs and VDEs Obtained by Experimental Measurements[a]

cluster		RE	VDE^{theo}	ADE^{theo}	VDE^{exp}	ADE^{exp}
VC_2^-	**1A**	0	1.33	1.23	1.56	1.29
	1B	0.23	1.02	1.00		
	1C	0.26	1.89	0.96		
$V_2C_2^-$	**2A**	0	1.50	1.44	1.47	1.17
	2B	0.41	1.32	1.22		
$V_3C_2^-$	**3A**	0	0.94	0.83	1.32	0.90
	3B	0.008	0.92	0.87		
	3C	0.01	1.12	1.00		
	3D	0.02	0.90	0.86		
	3E	0.28	0.57	0.55		
$V_4C_2^-$	**4A**	0	1.33	1.24	1.28	1.04
	4B	0.26	0.96	0.94		
	4C	0.27	1.14	1.13		
	4D	0.27	0.99	0.98		
$V_5C_2^-$	**5A**	0	1.26	1.20	1.14	0.94
	5B	0.06	0.96	0.92		
	5C	0.09	1.45	1.24		
	5D	0.16	0.82	0.82		
	5E	0.23	0.97	0.96		
$V_6C_2^-$	**6A**	0	1.07	1.05	1.29	1.05
	6B	0.17	1.25	1.15		
	6C	0.19	1.01	1.01		
	6D	0.19	1.02	1.02		
	6E	0.30	1.16	1.11		

[a] The uncertainties of the experimental values are ±0.08 eV.

Table 2. Calculated Relative Energies (REs), VDEs, and ADEs (eV) of the Low-Energy Structures of $V_nC_4^-$ (n = 1−6) Clusters as Well as Their ADEs and VDEs Obtained by Experimental Measurements[a]

cluster		RE	VDE^{theo}	ADE^{theo}	VDE^{exp}	ADE^{exp}
VC_4^-	**1a**	0	1.95	1.73	1.83	1.46
	1b	0.30	1.72	1.42		
$V_2C_4^-$	**2a**	0	2.36	2.10	2.06	1.90
	2b	0.18	1.95	1.92		
	2c	0.19	2.61	2.16		
	2d	0.42	2.04	1.98		
$V_3C_4^-$	**3a**	0	1.68	1.56	1.62	1.35
	3b	0.29	1.61	1.31		
	3c	0.34	1.21	1.37		
$V_4C_4^-$	**4a**	0	1.42	1.35	1.29	1.05
	4b	0.33	1.31	1.22		
	4c	0.42	1.29	1.12		
$V_5C_4^-$	**5a**	0	1.21	1.18	1.53	1.26
	5b	0.03	1.35	1.33		
	5c	0.16	1.33	1.29		
	5d	0.30	0.88	1.87		
$V_6C_4^-$	**6a**	0	1.33	1.26	1.56	1.24
	6b	0.01	1.33	1.25		
	6c	0.09	1.49	1.44		
	6d	0.18	1.34	1.29		
	6e	0.18	1.40	1.37		

[a] The uncertainties of the experimental values are ±0.08 eV.

DOI: 10.1021/acs.jpca.6b00241

Photoelectron Spectra of $V_nC_4^-$ (n = 1−6). The 266 nm spectrum of VC_4^- displays a broad peak centered at about 1.83 eV, a shoulder peak at 2.08 eV, followed by a relatively weak peak at 2.68 eV, and a very broad feature in the range of 3.0−4.0 eV. The 266 nm spectrum of $V_2C_4^-$ exhibits a weak peak at 2.06 eV and a much broader feature at 2.85 eV. There are also some unresolved peaks in the range of 3.0−4.0 eV. The 266 nm spectrum in this work is in reasonable agreement with the 355 nm spectrum of $V_2C_4^-$ reported by Tono et al.[21] For $V_3C_4^-$, the 266 nm spectrum shows three discernible peaks centered at 1.62, 2.13, and 3.04 eV, with a peak following at the higher binding energy of above 3.9 eV. The 266 nm spectrum of $V_4C_4^-$ displays four resolved peaks centered at 1.29, 1.96, 2.46, and 3.29 eV. There is an intense peak centered at 1.53 eV in the 266 nm spectrum of $V_5C_4^-$. There are also several peaks at higher binding energies of about 1.75, 2.03, and 2.72 eV. In the 266 nm spectrum of $V_6C_4^-$, there is a peak centered at 1.56 eV and a broad band in the range of 2.05−3.26 eV.

It is worth mentioning that the photoelectron spectra of VC_4^-, $V_2C_4^-$, $V_3C_4^-$, and $V_4C_4^-$ have been reported in ref 23. The spectra of VC_4^- in this work are similar to that in ref 23 while those of $V_2C_4^-$, $V_3C_4^-$, and $V_4C_4^-$ are very different from those in ref 23. That is probably because the spectra in ref 23 were contaminated by impurities due to low mass resolution.

4. COMPUTATIONAL RESULTS

The open 3d shells of vanadium result in many low-energy isomers. These low-energy isomers are valuable to assign the observed spectra and to understand the growth mechanisms of the related vanadium carbide nanoclusters. Therefore, the lowest-energy isomers and several low-energy isomers of anionic $V_nC_2^-$ and $V_nC_4^-$ (n = 1−6) clusters are shown in Figures 2 and 3, in which relative energies and symmetries are also presented. The lowest-energy geometries and symmetries of neutral V_nC_2 and V_nC_4 (n = 1−6) are shown in Figure 4. The calculated ADE and VDE values of anionic $V_nC_2^-$ and $V_nC_4^-$ (n = 1−6) clusters are listed in Tables 1 and 2, respectively.

Anionic $V_nC_2^-$ (n = 1−6). The lowest-energy isomer of VC_2^- (1A) was calculated to be an isosceles triangular structure with $^5B_1$ electronic state. The C−C and C−V bond lengths of isomer 1A were calculated to be 1.30 and 2.00 Å, respectively. Isomer 1B is an isosceles triangular structure with triplet state. It is higher in energy than isomer 1A by 0.23 eV. Isomer 1C has a linear V−C−C configuration, which is similar to the linear structure of CrC_2^- anion reported in the literature.[35] It is higher in energy than isomer 1A by 0.26 eV. The VDE and ADE of isomer 1A were calculated to be 1.33 and 1.23 eV, respectively, which are much closer to the experimental measurements (1.56 and 1.29 eV) than those of isomer 1B (1.02 and 1.00 eV) and isomer 1C (1.89 and 0.96 eV). Thus, the most probable ground state isomer of VC_2^- is an isosceles triangular structure with $^5B_1$ electronic state, which is in line with calculations at the DFT/B3LYP level.[36]

For $V_2C_2^-$, the lowest-energy structure (isomer 2A) has a four-membered ring geometry with $^2A''$ electronic state. The C−C and V−V bond lengths were calculated to be 1.31 and 1.81 Å, respectively. Isomer 2B has a structure similar to isomer 2A, but it is in the ^4A state. It is higher in energy than isomer 2A by 0.41 eV. The calculated VDE of isomer 2A (1.50 eV) is closer to the experimental value (1.47 eV) than that of isomer 2B (1.32 eV). As a result, we suggest that the four-membered ring geometry (isomer 2A) with $^2A''$ electronic state is the most probable ground state structure of $V_2C_2^-$. This is in agreement with the results of Tono et al.[20]

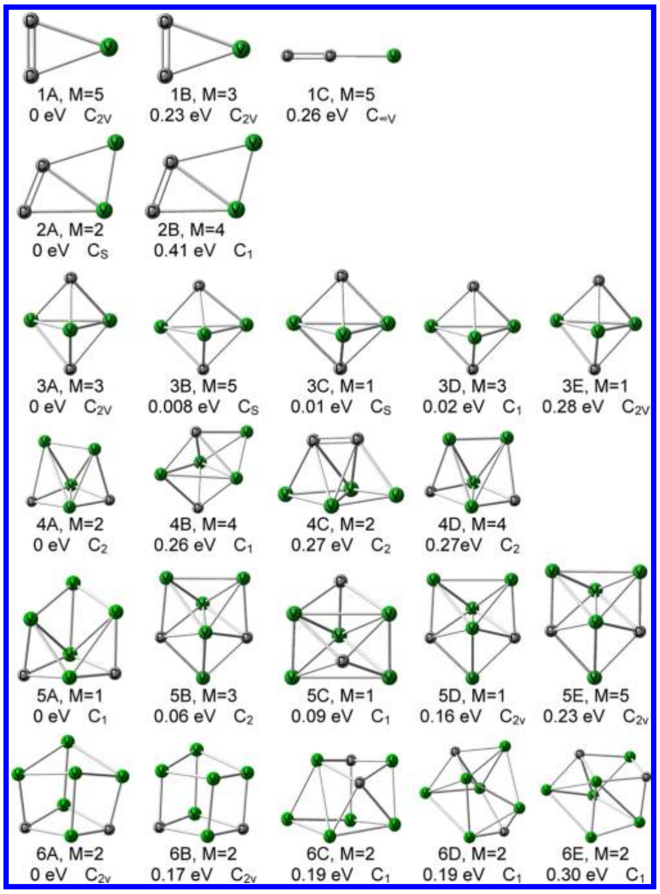

Figure 2. Geometries of the low-energy isomers of anionic $V_nC_2^-$ (n = 1−6), as well as their relative energies and spin multiplicities (M).

The geometric features of the lowest-energy structure of $V_3C_2^-$ (isomer 3A) are greatly different from those of VC_2^- and $V_2C_2^-$. It is a trigonal bipyramidal structure with two separate carbon atoms attached to the triangular V_3. Isomers 3B, 3C, and 3D are degenerate in energy with isomer 3A. They have similar geometries to isomer 3A but with different spin states. Isomers 3B−3D are higher in energy than isomer 3A by only 0.008, 0.01, and 0.02 eV. Isomer 3E is higher in energy than isomer 3A by 0.28 eV. Isomers 3A−3D are almost degenerate in energy and their VDEs and ADEs are all close to the experimental values. Therefore, isomers 3A−3D are all possible species generated in photoelectron spectroscopy experiments. This may be why the first peak in the photoelectron spectrum of $V_3C_2^-$ has a broad shoulder peak.

The lowest energy geometry of $V_4C_2^-$ (isomer 4A) consists of two separate carbon atoms attached to two faces of a distorted tetrahedral V_4 cluster. Isomer 4B is composed of a V atom attached to one face of $V_3C_2^-$. It is higher in energy than isomer 4A by 0.26 eV. Both isomers 4C and 4D are higher in energy than isomer 4A by 0.27 eV. Isomer 4C consists of a carbon dimer attached to a quasi-planar four-membered ring V_4 cluster. Isomer 4D has a similar structure to isomer 4A (^2B electronic state), but it is in a different electronic state (^4A). The calculated VDE and ADE of isomer 4A are 1.33 and 1.24 eV, respectively, which are in good agreement with the experimental values (1.28 and 1.04 eV). Thus, isomer 4A is

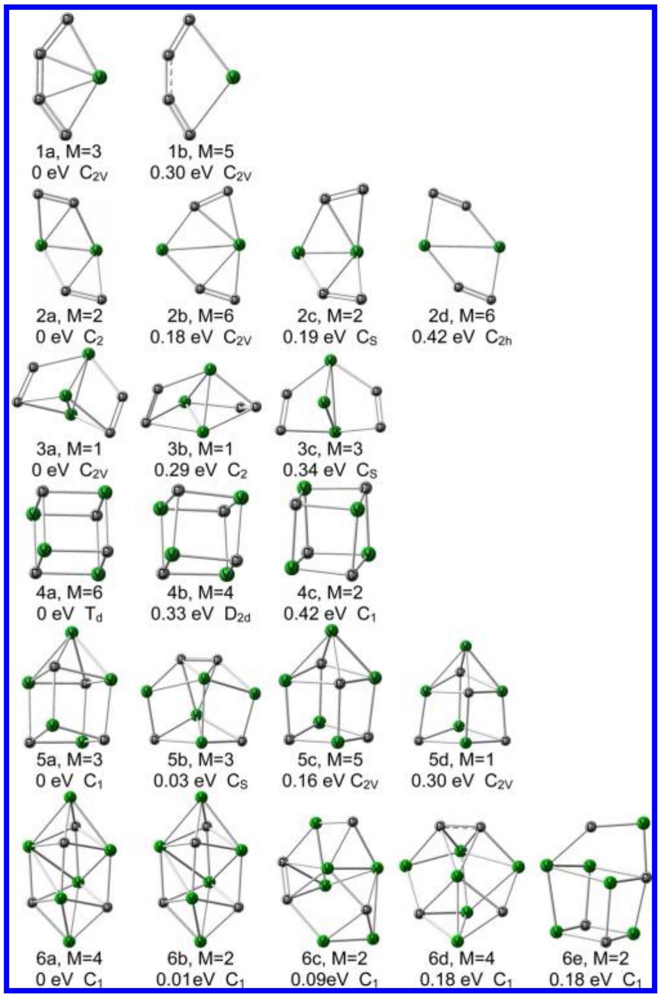

Figure 3. Geometries of the low-energy isomers of anionic $V_nC_4^-$ (n = 1−6), as well as their relative energies and spin multiplicities (M).

the most probable structure of the $V_4C_2^-$ cluster generated in the experiment.

The lowest-energy structure of anionic $V_5C_2^-$ (isomer 5A) is composed of two separate carbon atoms attached to two faces of a distorted triangular bipyramidal V_5 cluster. Isomer 5B has two vanadium atoms attached to two faces of a V_3C_2 trigonal bipyramid. It is higher in energy than isomer 5A by only 0.06 eV. Isomer 5C is composed of two separate carbon atoms attached to the surfaces of a three-membered and four-membered ring of a distorted rectangular pyramid of V_5. It is higher in energy than isomer 5A by 0.09 eV. Isomers 5D and 5E have similar geometries to isomer 5B. They are higher in energy than isomer 5A by 0.16 and 0.23 eV. The electronic states of isomers 5B, 5D, and 5E are ^3B, $^1A_1$, and $^5B_2$, respectively. The VDEs of isomers 5A and 5B are 1.26 and 0.96 eV, and both are close to the experimental value of 1.14 eV. In addition, their energy difference is only 0.06 eV. Therefore, it is possible that isomers 5A and 5B are both generated in the cluster experiment. The calculated VDE of isomer 5C is about 1.45 eV. It may contribute to the high EBE features in the experimental spectrum.

Similar to the geometric characteristics of $V_nC_2^-$ (n = 3−5) clusters, it is also two separate carbon atoms interacting with an octahedral V_6 cluster in the lowest energy structure (isomer 6A) of anionic $V_6C_2^-$. Isomers 6B−6E are higher in energy than isomer 6A by 0.17, 0.19, 0.19, and 0.30 eV, respectively. They all consist of two separate carbon atoms interacting with vanadium clusters. The ADE and VDE of isomer 6A were calculated to be 1.05 and 1.07 eV, which are close to the experimental measurements (1.05 and 1.29 eV). Consequently, isomer 6A is the most probable structure of $V_6C_2^-$ cluster produced in the cluster experiment.

Neutral V_nC_2 (n = 1−6). The lowest-energy isomer of neutral VC_2 is a C_{2v} triangular structure with $^4B_1$ electronic state, which is in agreement with the results of a previous study.[36] The lowest-energy isomer of neutral V_2C_2 is a four-membered ring structure with $^1A'$ electronic state, which is consistent with the DFT calculated result by Tono et al.[20] The lowest-energy geometry of neutral V_3C_2 is a trigonal bipyramidal structure. The lowest energy isomer of neutral V_4C_2 is composed of a V atom attached to one surface of a V_3C_2 trigonal bipyramid. We also found another isomer similar to the lowest-energy geometry of anionic V_4C_2. It is higher in energy than the lowest-energy geometry of V_4C_2 by only 0.04 eV (Figure S1, Supporting Information). The lowest-energy geometry of neutral V_5C_2 comprises a vanadium dimer attached to the two triangular faces of a V_3C_2 cluster. The lowest-energy structure of neutral V_6C_2 consists of two separate carbon atoms interacting with an octahedral V_6 cluster. By comparing the neutral V_nC_2 (n = 1−6) clusters with the corresponding anionic species, it is found that the structures of neutral VC_2, V_2C_2, V_3C_2, and V_6C_2 are similar to their corresponding anionic species, while the structures of neutral V_4C_2 and V_5C_2 are different from their corresponding anionic species.

Anionic $V_nC_4^-$ (n = 1−6). The lowest energy structure of anionic VC_4^- (isomer 1a) has a fan-like configuration with the V interacting with a C_4 chain. It is worth mentioning that the fan-like ground state structure of VC_4^- anion is different from the linear structure of CrC_4^- anion in the literature.[35] The electronic state of isomer 1a is $^3B_1$. Isomer 1b is also a fan-like structure but with $^5B_2$ electronic state. The VDE of isomer 1a

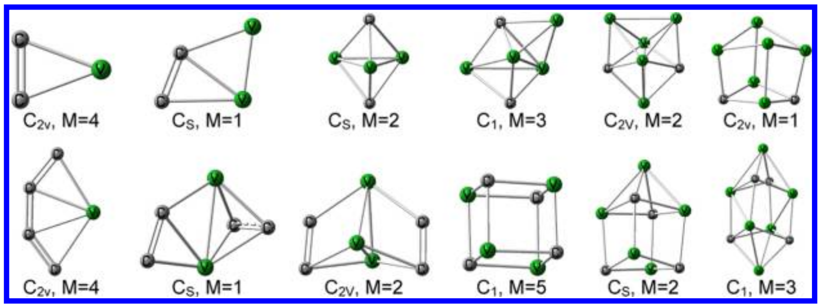

Figure 4. Lowest-energy geometries and symmetries of neutral V_nC_2 and V_nC_4 (n = 1−6), as well as their spin multiplicities (M).

was calculated to be 1.95 eV at BPW91 level, close to the experimental measurement (1.83 eV). The VDE of isomer 1b was calculated to be 1.72 eV, but isomer 1b is much less stable than isomer 1a by 0.30 eV. Thus, isomer 1a is the most probable one detected in the experiments.

The lowest-energy structure of anionic $V_2C_4^-$ (isomer 2a) is composed of two four-membered $V_2C_2^-$ rings with a shared V—V bond, in which two C_2 units are parallel to the V—V bond. It has a similar non-planar structure to the ground state structures of $Nb_2C_4^-$ and $Ti_2C_4^+$.[37,38] The two C—C bond lengths are both 1.31 Å, which are close to that of the free ethylene (1.33 Å). The four V—C bonds are all 2.02 Å. Isomer 2b was calculated to be 0.18 eV higher in energy than isomer 2a. It is a planar six-membered ring structure with two C_2 units on the two sides of the V—V bond. Isomer 2c is a nonplanar six-membered ring structure with two C_2 units bridged by V_2. It is higher in energy than isomer 2a by 0.19 eV. Isomer 2d is higher in energy than isomer 2a by 0.42 eV. It consists of a planar six-membered cycle with two four-membered rings of V_2C_2 sharing one V—V bond. The ADE and VDE of isomer 2a were calculated to be 2.10 and 2.36 eV, respectively, which are in agreement with the experimental measurements (1.90 and 2.06 eV). Thus, isomer 2a is the most stable structure of the $V_2C_4^-$ cluster. Tono et al. reported a structure with two vertical C_2 units on the two sides of the shared V—V bond to be the most stable structure of anionic $V_2C_4^-$.[21] We calculated this structure to be 0.51 eV higher in energy than the lowest energy structure (Figure S1, Supporting Information). Knappenberger et al. also calculated it to be higher in energy by 0.38 eV than their most stable isomer. They reported that the most stable structure of anionic $V_2C_4^-$ is made up of two four-membered $V_2C_2^-$ cycles with a shared V—V bond,[23] which is similar to isomer 2b in this work.

The lowest-energy structure of anionic $V_3C_4^-$ (isomer 3a) consists of two C_2 units attached to the surface of a triangular V_3 cluster, in which the two C═C bonds are parallel. Isomer 3b is also composed of two C_2 units attached to the two sides of a triangular V_3 cluster, in which the two C═C bonds are crossed with each other. It is higher in energy than isomer 3a by 0.29 eV. Isomer 3c is higher in energy than isomer 3a by 0.34 eV. It has a similar configuration to isomer 3a. The electronic states of isomers 3a and 3c are ^1A and $^3A''$. The ADE and VDE of isomer 3a were calculated to be 1.56 and 1.68 eV, respectively, which are in reasonable agreement with experimental measurements (1.35 and 1.62 eV). Thus, isomer 3a is the most probable structure of $V_3C_4^-$ detected in the experiment.

The lowest-energy geometry of anionic $V_4C_4^-$ (isomer 4a) is a cubic structure, which is similar to the structures of early transition metal carbides, such as $Nb_4C_4^{0/+}$ and Ti_4C_4 clusters.[38−40] The geometries of isomers 4b and 4c are similar to that of isomer 4a. They are higher in energy than isomer 4a by 0.33 and 0.42 eV, respectively. The electronic states of isomers 4a, 4b, and 4c are $^6A_1$, $^4B_2$, and ^2A, respectively. The calculated ADE and VDE of isomer 4a are 1.35 and 1.42 eV, respectively, which are close to the experimental values (1.05 and 1.29 eV). As a result, isomer 4a is the most probable structure of $V_4C_4^-$ detected in the experiment.

The lowest-energy structure of anionic $V_5C_4^-$ (isomer 5a) is composed of a vanadium atom capping the cubic structure of anionic $V_4C_4^-$. Isomer 5b consists of two separate carbon atoms attached to two three-membered V_3 rings and one C_2 unit attached to one four-membered V_4 ring of a distorted triangular bipyramidal V_5 cluster. It is higher in energy than isomer 5a by only 0.03 eV. Isomers 5c and 5d are higher in energy than isomer 5a by 0.16 and 0.30 eV, respectively. They have similar structures to isomer 5a. The VDEs of isomers 5a and 5b were calculated to be 1.21 and 1.35 eV, both in agreement with the experimental measurement (1.53 eV). In addition, the energy separation of isomers 5a and 5b is only 0.03 eV. Thus, we suggest that isomers 5a and 5b may both be generated in the cluster experiment.

The first two lowest-energy structures of anionic $V_6C_4^-$ (isomers 6a and 6b) are composed of two vanadium atoms capping the cubic structure of anionic $V_4C_4^-$. Isomers 6b and 6c are higher in energy than isomer 6a by 0.01 and 0.09 eV, respectively. Isomers 6d and 6e are both higher in energy than isomer 6a by 0.18 eV. The calculated ADEs and VDEs of isomers 6a−6c are all close to the experimental measurements (1.24 and 1.56 eV). In addition, they are almost degenerate in energy. Thus, we suggest that isomers 6a−6c may all be generated in the cluster experiment. This explains why the first peak of $V_6C_4^-$ is very broad in the photoelectron spectrum.

Neutral V_nC_4 (n = 1−6). The lowest-energy structure of neutral VC_4 has a fan-like configuration with $^4B_1$ electronic state, which is in agreement with the lowest-energy fan-like structure reported by Redondo et al.[17] The lowest-energy structure of neutral V_2C_4 comprises two V_2C_2 four-membered cycles sharing one V—V bond with two vertical C═C bonds. The lowest-energy structure of neutral V_3C_4 comprises two C_2 units adsorbed on both sides of the triangular V_3 cluster, in which the two C═C bonds are parallel. Another nearly degenerate isomer is 0.04 eV higher in energy than the lowest-energy isomer of neutral V_3C_4, which is similar to the second most stable isomer of anionic $V_3C_4^-$ (isomer 3b) (Figure S1, Supporting Information). The lowest-energy structure of neutral V_4C_4 has a cubic configuration with carbon and vanadium atoms alternatively aligned. The lowest-energy structure of neutral V_5C_4 consists of a vanadium atom capping the cubic structure of V_4C_4. The lowest-energy structure of neutral V_6C_4 consists of two vanadium atoms capping the cubic structure of V_4C_4. From Figures 3 and 4, one can see that the structures of neutral VC_4, V_3C_4, V_4C_4, V_5C_4, and V_6C_4 clusters are similar to those of their corresponding anionic species while the structure of neutral V_2C_4 is very different from that of anionic V_2C_4.

5. DISCUSSION

Binding Energies of $V_nC_2^{-/0}$ and $V_nC_4^{-/0}$ (n = 1−6). To further investigate the relative stabilities of the $V_nC_2^{-/0}$ and $V_nC_4^{-/0}$ (n = 1−6) clusters, we calculated the binding energies (E_bs) per atom for the lowest-energy structures of these clusters. The E_b values of the $V_nC_2^{-/0}$ and $V_nC_4^{-/0}$ (n = 1−6) clusters were calculated according to the following definitions:

$$E_b(V_nC_m) = [nE(V) + mE(C) - E(V_nC_m)]/(n + m) \quad (1)$$

$$E_b(V_nC_m^-) = [nE(V) + (m - 1)E(C) + E(C^-) - E(V_nC_m^-)]/(n + m) \quad (2)$$

The $E(V)$, $E(C^{-/0})$, and $E(V_nC_m)^{-/0}$ are the total energies of the most stable V, $C^{-/0}$, and $V_nC_m^{-/0}$ clusters, respectively. Because the electron affinity of the carbon atom (1.26 eV)[41] is higher than that of the vanadium atom (0.53 eV),[42] we made the negative charge on a carbon atom in eq 2. The E_b values of the $V_nC_2^{-/0}$ and $V_nC_4^{-/0}$ clusters are shown in Table 3. One can see that the E_b values of the anionic and neutral V_nC_2 and V_nC_4 (n = 1−6) clusters all decrease with increasing cluster size n. This indicates that the stability of anionic and neutral V_nC_2 and V_nC_4 (n = 1−6) clusters decreases with increasing vanadium cluster size n. It is interesting to note that the E_b values of $V_nC_4^{-/0}$ (n = 1−6) are always higher than those of the corresponding $V_nC_2^{-/0}$ (n = 1−6) counterparts. This reveals that carbon-rich $V_nC_4^{-/0}$ (n = 1−6) clusters are more stable than carbon-deficient $V_nC_2^{-/0}$ (n = 1−6) clusters. This stability mainly depends on the bond types of the clusters that the C=C double bond (7.03 eV) is much stronger than the V−C bond (4.83 eV) and the V−C bond is much stronger than the V−V bond (2.49 eV).[43] The E_b values of neutral V_nC_2 and V_nC_4 (n = 1−6) clusters are higher than those of their corresponding anionic counterparts. This reveals that the stabilities of neutral V_nC_2 and V_nC_4 (n = 1−6) clusters are higher than those of their corresponding anionic counterparts.

Table 3. Binding Energies of $V_nC_2^{0/-}$ and $V_nC_4^{0/-}$ (n = 1−6) Clusters

cluster	E_b^-	E_b^0	cluster	E_b^-	E_b^0
VC_2	4.83	5.34	VC_4	6.38	6.59
V_2C_2	4.52	4.86	V_2C_4	6.00	6.13
V_3C_2	4.22	4.59	V_3C_4	5.66	5.84
V_4C_2	4.19	4.45	V_4C_4	5.54	5.72
V_5C_2	4.11	4.37	V_5C_4	5.27	5.45
V_6C_2	4.05	4.26	V_6C_4	5.09	5.24

NPA of Neutral V_nC_2 and V_nC_4 (n = 1−6). The total NPA charge distributions on all carbon atoms and C−C Wiberg bond orders are listed in Table 4. From Table 4, one can see that the charges on the carbon units for neutral V_nC_2 and V_nC_4 (n = 1−6) clusters are all negative. This reveals that electrons always transfer from vanadium clusters to carbon units, which is because the electron affinities of C, C_2, and C_4 are much higher than those of V_n (n = 1−6) clusters.[41,42,44−46] The average charges on each carbon atom of neutral V_nC_2 and V_nC_4 (n = 1−6) clusters are −0.351, −0.304, −0.427, −0.464, −0.425, −0.291 and −0.198, −0.253, −0.311, −0.272, −0.279, −0.350, which reveal that V−C in these clusters are covalent bonds. The C−C bond orders of VC_2 and V_2C_2 are 2.09 and 2.07, while those of V_3C_2−V_6C_2 are 0.17, 0.09, 0.05, and 0.05, respectively. This indicates that the two carbon atoms form the C−C double bond in VC_2 and V_2C_2 clusters, whereas no C−C bond is formed in $V_{3-6}C_2$. The C−C bond orders of VC_4, V_2C_4, and V_3C_4 are 2.08, 1.99, and 1.87, while those of V_4C_4, V_5C_4, and V_6C_4 are 0.04, 0.07, and 0.07, respectively. This shows that for V_nC_4 (n = 1−6) clusters, the C−C bonds have double-bond characteristics for n = 1−3, while the carbon atoms are separated by the vanadium atoms for n = 4−6. The V−C bond orders are in the range of 0.82−1.44, indicating that V−C single bonds exist in V_nC_2 and V_nC_4 (n = 1−6) clusters. Comparing the largest V−V bond orders of V_nC_2 (n = 2−6) with those of V_nC_4 (n = 2−6), one can see that the former are always higher than the latter. This is mainly because increasing the carbon number weakens the V−V interaction. In addition, the V−V bond orders in Table 4 show that multiple metal bonds exist in V_nC_2 and V_nC_4 (n = 1−6) except for V_4C_4 and V_6C_4.

Spin Multiplicities of $V_nC_2^{-/0}$ and $V_nC_4^{-/0}$ (n = 1−6). The consideration of spin multiplicities is essential for transition metal-containing clusters due to their unfilled *d* orbitals. Spin multiplicities of the lowest-energy isomers of anionic V_nC_2 and V_nC_4 (n = 1−6) are 5, 2, 3, 2, 1, 2 and 3, 2, 1, 6, 3, 4, while spin multiplicities of the lowest-energy isomers of neutral V_nC_2 and V_nC_4 (n = 1−6) are 4, 1, 2, 3, 2, 1 and 4, 1, 2, 5, 2, 3, respectively. In view of these spin multiplicities, one can see that $V_4C_4^{-/0}$ clusters have the highest spin states among these clusters. Perhaps it arises from their special cubic structures, as we all known that the material's properties depend on the geometric structures greatly. We can also suggest that magnetic moments of $V_4C_4^{-/0}$ clusters are the highest among the $V_nC_2^{-/0}$ and $V_nC_4^{-/0}$ (n = 1−6) clusters, which indicates that V_4C_4 may be a good candidate for magnetic materials.

Structural Evolution of $V_nC_2^{-/0}$ and $V_nC_4^{-/0}$ (n = 1−6). Geometric evolution is important for cluster-assembled nanomaterials. For the $V_nC_2^{-/0}$ clusters (Figures 2 and 4), it was found that the two carbon atoms directly interact with each other to form a carbon dimer for n = 1 and 2 while the two carbon atoms are separated by the V clusters for n = 3−6. For the $V_nC_4^{-/0}$ clusters (Figures 3 and 4), the four carbon atoms form a C_4 chain for n = 1 and they form two C=C double bonds for n = 2 and 3, whereas the four carbon atoms are completely separated by V atoms for n = 4−6. Generally, vanadium clusters in $V_nC_2^{-/0}$ (n = 1−6), as an integral cluster unit, interact with C_2 unit or two separate C atoms. For $V_nC_4^{-/0}$ (n = 1−6), the vanadium atom interacts with a C_4 chain for n = 1, followed by the vanadium clusters interacting with two C_2 units for n = 2 and 3, and then vanadium clusters and four carbon atoms are completely separated by the opposite side for n = 4; after that, one or two vanadium atoms cap on the cubic V_4C_4 cluster for n = 5 or 6.

The geometric evolution of $V_nC_2^{-/0}$ and $V_nC_4^{-/0}$ (n = 1−6) clusters demonstrates that separate carbon atoms interact with separate vanadium atoms when the vanadium number is greater than or equal to the carbon number, whereas a carbon dimer or tetramer interacts with vanadium clusters when the vanadium number is less than or equal to the carbon number. Increasing the V_n/C_2 and V_n/C_4 ratios will favor the diffusion between the carbon phase and the vanadium phase. As a result, we suggest that the vanadium−carbon ratio is one of the predominant

Table 4. NPA Charge on All Carbon Atoms (C^{charge}, e) in Neutral V_nC_2 and V_nC_4 (n = 1−6) Clusters as Well as Their Largest C−C, V−C, and V−V Bond Orders

cluster	C^{charge}	C−C	V−C	V−V	cluster	C^{charge}	C−C	V−C	V−V
VC_2	−0.701	2.09	1.18		VC_4	−0.789	2.08	0.82	
V_2C_2	−0.608	2.07	0.92	3.78	V_2C_4	−1.011	1.99	1.18	1.67
V_3C_2	−0.853	0.17	1.16	1.84	V_3C_4	−1.245	1.87	0.85	1.55
V_4C_2	−0.927	0.09	1.44	2.15	V_4C_4	−1.086	0.04	1.35	0.39
V_5C_2	−0.849	0.05	1.07	1.46	V_5C_4	−1.117	0.07	1.38	1.44
V_6C_2	−0.582	0.05	1.19	1.64	V_6C_4	−1.400	0.07	1.16	1.06

factors to control the formation type of vanadium carbides. Recently, Wang and co-workers found that a two-dimensional sheet of TiC_2 can be formed when the ratio of carbon increases, in which C_2 dimers act as the basic structural units rather than the individual carbon atoms.[47] The properties of the two-dimensional sheet of TiC_2 are different from those of MXenes in which carbon atoms exist individually. This indicates that the metal−carbon ratio is indeed an important parameter for tuning the properties of metal-carbides.

Structural Comparison of $V_nC_2^{-/0}$ and $Co_nC_2^{-/0}$ (n = 1−5). We have previously investigated $Co_nC_2^{-/0}$ (n = 1−5) clusters using photoelectron spectroscopy and DFT calculations.[30] It is noted that the geometries of $V_nC_2^{-/0}$ are similar to those of $Co_nC_2^{-/0}$ for n = 1 and 2, whereas they are very different for n = 3−5. In the geometries of $Co_nC_2^{-/0}$ (n = 3−5), the two carbon atoms form a carbon dimer, possessing the features of a C═C double bond. In contrast, in the geometries of $V_nC_2^{-/0}$ (n = 3−5), two separate carbon atoms interact with the vanadium clusters. This geometric discrepancy may originate from the different valence electrons of V ($3d^34s^2$) and Co ($3d^74s^2$). It may also arise from different metal atom radius of V (1.34 Å) and Co (1.25 Å), as reported by Helden et al. that metal carbides can be considered as the octahedral holes of a regular metal lattice intercalated by carbon atoms when metal atom radius is above 1.3 Å, or otherwise not.[48] It is interesting to find this geometric difference between $V_nC_2^{-/0}$ and $Co_nC_2^{-/0}$ (n = 3−5). It is possible that this kind of geometric distinction reveals the different carbide-formation mechanisms of the late and the early 3d transition metals, which may be one of the reasons the two-dimensional carbide materials, also known as MXene, are formed by early transition metal carbides, rather than late transition metal carbides.

6. CONCLUSIONS

The geometric and electronic structures of $V_nC_2^{-/0}$ and $V_nC_4^{-/0}$ (n = 1−6) clusters were investigated using density functional theory calculations. The adiabatic and vertical detachment energies of $V_nC_2^-$ and $V_nC_4^-$ (n = 1−6) clusters were measured from photoelectron spectroscopy experiments. The most stable structures of $V_nC_2^{-/0}$ and $V_nC_4^{-/0}$ (n = 1−6) were determined by combining the experimental and theoretical results. The geometric evolution of $V_nC_2^{-/0}$ and $V_nC_4^{-/0}$ (n = 1−6) clusters indicates that the V_n/C_m ratio is one of the predominant factors to control the formation type of vanadium carbide clusters. To some extent, the V_n/C_m ratio will favor the diffusion of the carbon phase and vanadium phase. The binding energies reveal that the stabilities of $V_nC_2^{0/-}$ and $V_nC_4^{0/-}$ (n = 1−6) clusters decrease with increasing vanadium number whereas their stabilities increase with increasing carbon number.

■ ASSOCIATED CONTENT

Supporting Information

The Supporting Information is available free of charge on the ACS Publications website at DOI: 10.1021/acs.jpca.6b00241.

Comparisons of the ADEs and VDEs (eV) of $V_nC_2^-$ (n = 1−2) for the different functionals (BPW91, B3LYP, and PBE) and all-electron basis set 6-311+G(d) and the pseudopotential basis set TZVP. The low-energy isomers of anionic $V_2C_4^-$, $V_6C_4^-$, and the degenerate energy isomers of neutral V_4C_2 and V_3C_4 clusters. The mass spectrum of $V_mC_n^{0/-}$ (m = 1−6, n = 2, 4). Cartesian coordinates of the low-energy isomers of $V_nC_2^{0/-}$ and $V_nC_4^{0/-}$ (n = 1−6). (PDF)

■ AUTHOR INFORMATION

Corresponding Authors

*E-mail: jlyang@ustc.edu.cn.
*E-mail: zhengwj@iccas.ac.cn.

Notes

The authors declare no competing financial interest.

■ ACKNOWLEDGMENTS

The authors acknowledge the National Natural Science Foundation of China (21401064), the Open research fund of Beijing National Laboratory for Molecular Sciences (20140164), the China Postdoctoral Science Foundation (2015M580537) and the Natural Science Foundation of the Education Department of Henan Province (15A150060) for support. We are grateful to Professor Zhen Gao for discussion.

■ REFERENCES

(1) Levy, R. B.; Boudart, M. Platinum-like Behavior of Tungsten Carbide in Surface Catalysis. *Science* **1973**, *181*, 547−549.

(2) Tang, Q.; Zhou, Z.; Shen, P. Are MXenes Promising Anode Materials for Li Ion Batteries? Computational Studies on Electronic Properties and Li Storage Capability of Ti_3C_2 and $Ti_3C_2X_2$ (X = F, OH) Monolayer. *J. Am. Chem. Soc.* **2012**, *134*, 16909−16916.

(3) Naguib, M.; Come, J.; Dyatkin, B.; Presser, V.; Taberna, P.-L.; Simon, P.; Barsoum, M. W.; Gogotsi, Y. MXene: A Promising Transition Metal Carbide Anode for Lithium-ion Batteries. *Electrochem. Commun.* **2012**, *16*, 61−64.

(4) Wei, S.; Guo, B. C.; Purnell, J.; Buzza, S.; Castleman, A. W., Jr. Metallocarbohedrenes as a Class of Stable Neutral Clusters: Formation Mechanism of M_8C_{12} (M = Ti and V). *J. Phys. Chem.* **1992**, *96*, 4166−4168.

(5) Pilgrim, J. S.; Duncan, M. A. Metallo-Carbohedrenes: Chromium, Iron, and Molybdenum Analogues. *J. Am. Chem. Soc.* **1993**, *115*, 6958−6961.

(6) Wei, S.; Guo, B. C.; Purnell, J.; Buzza, S.; Castleman, A. W., Jr. Metallo-Carbohedrenes: Formation of Multicage Structures. *Science* **1992**, *256*, 515.

(7) Naguib, M.; Kurtoglu, M.; Presser, V.; Lu, J.; Niu, J.; Heon, M.; Hultman, L.; Gogotsi, Y.; Barsoum, M. W. Two-Dimensional Nanocrystals Produced by Exfoliation of Ti_3AlC_2. *Adv. Mater.* **2011**, *23*, 4248−4253.

(8) Naguib, M.; Mochalin, V. N.; Barsoum, M. W.; Gogotsi, Y. 25th Anniversary Article: A New Family of Two-Dimensional Materials. *Adv. Mater.* **2014**, *26*, 992−1005.

(9) Zou, Z.; Fu, L.; Song, X.; Zhang, Y.; Liu, Z. Carbide-Forming Groups IVB-VIB Metals: A New Territory in the Periodic Table for CVD growth of Graphene. *Nano Lett.* **2014**, *14*, 3832−3839.

(10) Bethune, D. S.; Klang, C. H.; De Vries, M. S.; Gorman, G.; Savoy, R.; Vazquez, J.; Beyers, R. Cobalt-catalysed Growth of Carbon Nanotubes with Single-Atomic-Layer Walls. *Nature* **1993**, *363*, 605−607.

(11) Clemmer, D. E.; Hunter, J. M.; Shelimov, K. B.; Jarrold, M. F. Physical and Chemical Evidence for Metallofullerenes with Metal Atoms as Part of the Cage. *Nature* **1994**, *372*, 248−250.

(12) Guo, B. C.; Wei, S.; Purnell, J.; Buzza, S.; Castleman, A. W., Jr. Metallo-Carbohedrenes $[M_8C_{12}^+$ (M = V, Zr, Hf, and Ti)]: A Class of Stable Molecular Cluster Ions. *Science* **1992**, *256*, 515−516.

(13) Pilgrim, J. S.; Duncan, M. A. Beyond Metallo-Carbohedrenes: Growth and Decomposition of Metal-carbon Nanocrystals. *J. Am. Chem. Soc.* **1993**, *115*, 9724−9727.

(14) von Helden, G.; van Heijnsbergen, D.; Duncan, M. A.; Meijer, G. IR-REMPI of Vanadium-Carbide Nanocrystals: Ideal versus Truncated Lattices. *Chem. Phys. Lett.* **2001**, *333*, 350−357.

(15) Yan, Z.; Cai, M.; Shen, P. K. An Ion Exchange Route to Produce Carbon Supported Nanoscale Vanadium Carbide for Electrocatalysis. *J. Mater. Chem.* **2011**, *21*, 19166−19170.

(16) Hu, J.; Xu, B.; Ouyang, C.; Yang, S. A.; Yao, Y. Investigation on V_2C and $V_2C_2X_2$ (X = F, OH) Monolayer as a Promising Anode Material for Li Ion Batteries from First-Principles Calculations. *J. Phys. Chem. C* **2014**, *118*, 24274−24281.

(17) Redondo, P.; Barrientos, C.; Largo, A. Small Carbon Clusters Doped with Vanadium Metals: a Density Functional Study of VC_n (n = 1−8). *J. Chem. Theory Comput.* **2006**, *2*, 885−893.

(18) Redondo, P.; Barrientos, C.; Largo, A. Structures and Stabilities of Non-linear $VC_n^{\pm}$ (n = 1−8) Clusters. *Int. J. Mass Spectrom.* **2007**, *263*, 101−112.

(19) Majumdar, D.; Roszak, S.; Balasubramanian, K. Electronic Structure and Spectroscopic Properties of Electronic States of VC_2, VC_2^-, and VC_2^+. *J. Chem. Phys.* **2003**, *118*, 130−141.

(20) Tono, K.; Terasaki, A.; Ohta, T.; Kondow, T. Geometric and Electronic Structures of $V_2C_2^-$ and V_2C_2 Studied by Photoelectron Spectroscopy and Density-functional Calculations. *Chem. Phys. Lett.* **2002**, *351*, 135−141.

(21) Tono, K.; Terasaki, A.; Ohta, T.; Kondow, T. Electronic and Geometric Structures of $Co_2V_n^-$ and $V_2C_n^-$: Initial Growth Mechanisms of Late and Early 3d Transition-metal Carbide Clusters. *J. Chem. Phys.* **2002**, *117*, 7010−7016.

(22) Kerns, K. P.; Guo, B. C.; Deng, H. T.; Castleman, A. W., Jr. Collision-Induced Dissociation of Vanadium-Carbon Cluster Cations. *J. Phys. Chem.* **1996**, *100*, 16817−16821.

(23) Knappenberger, K. L.; Jones, C. E.; Sobhy, M. A.; Iordanov, I.; Sofo, J.; Castleman, A. W., Jr. Anion Photoelectron Spectroscopy and Density Functional Investigation of Vanadium Carbide Clusers. *J. Phys. Chem. A* **2006**, *110*, 12814−12821.

(24) Xu, H.-G.; Zhang, Z.-G.; Feng, Y.; Yuan, J. Y.; Zhao, Y. C.; Zheng, W. J. Vanadium-doped Small Silicon Clusters: Photoelectron Spectroscopy and Density-functional Calculations. *Chem. Phys. Lett.* **2010**, *487*, 204−208.

(25) Becke, A. D. Density-functional Exchange-energy Approximation with Correct Asymptotic Behaviorl. *Phys. Rev. A: At., Mol., Opt. Phys.* **1988**, *38*, 3098−3100.

(26) Perdew, J. P.; Wang, Y. Accurate and Simple Analytic Representation of the Electron-Gas Correlation on Energy. *Phys. Rev. B: Condens. Matter Mater. Phys.* **1992**, *45*, 13244−13249.

(27) Frisch, M. J.; Trucks, G. W.; Chlegel, H. B.; Scuseria, G. E.; Robb, M. A.; Cheeseman, J. R.; Zakrzewski, V. G.; Montgomery, J. A.; Stratmann, R. E.; Burant, J. C.; et al. *Gaussian 09*; Gaussian, Inc.: Wallingford, CT, 2009.

(28) Gutsev, G. L.; Bauschlicher, C. W. Chemical Bonding, Electron Affinity, and Ionization Energies of the Homonuclear 3d Metal Dimers. *J. Phys. Chem. A* **2003**, *107*, 4755−4767.

(29) Guzmán-Ramírez, G.; Salvador, P.; Robles, J.; Vega, A.; Aguilera-Granja, F. Density Functional Study of ternary $Fe_xCo_yNi_z$ (x+y+z = 7) Clusters. *Theor. Chem. Acc.* **2013**, *132*, 1−12.

(30) Yuan, J. Y.; Xu, H.-G.; Zheng, W.-J. Photoelectron Spectroscopy and Density Functional Study of $Co_nC_2^-$ (n = 1−5) Clusters. *Phys. Chem. Chem. Phys.* **2014**, *16*, 5434−5439.

(31) Yuan, J. Y.; Yang, B. C.; Li, G. W.; Si, Y. B.; Wang, S. W.; Zhang, S. R.; Chen, H. Y. Geometries and Electronic Properties of Bimetallic CuV_n (n = 1−5) Clusters and Their Cations: Insight from Density Functional Calculations. *Comput. Mater. Sci.* **2015**, *102*, 213−219.

(32) Yuan, J. Y.; Li, G. W.; Yang, B. C.; Zhang, J. P.; Li, Z. J.; Chen, H. Y. Selective Adsorption of Ethylene on Bimetallic $CuV_n^{+/0}$ (n = 1−5) Clusters: a Theoretical Study. *Comput. Mater. Sci.* **2016**, *111*, 489−496.

(33) Reed, A. E.; Curtiss, L. A.; Weinhold, F. Intermolecular Interactions from a Natural Bond Orbital, Donor-Acceptor Viewpoint. *Chem. Rev.* **1988**, *88*, 899−926.

(34) Li, X.; Wang, L.-S. Electron Structure and Chemical Bonding between the First Row Transition Metals and C_2: A Photoelectron Spectroscopy Study of MC_2^- (M = Sc, V, Cr, Mn, Fe, and Co). *J. Chem. Phys.* **1999**, *111*, 8389−8395.

(35) Zhai, H. J.; Wang, L.-S.; Jena, P.; Gutsev, G. L.; Bauschlicher, C. W., Jr. Competition Between Linear and Cyclic Structures in Monochromium Carbide Clusters CrC_n^- and CrC_n (n = 2−8): a Photoelectron Spectroscopy and Density Functional Study. *J. Chem. Phys.* **2004**, *120*, 8996−9008.

(36) Rayón, V. M.; Redondo, P.; Barrientos, C.; Largo, A. Structures and Bonding in First-Row Transition-Metal Dicarbides: Are They Related to the Stability of Met-Cars? *Chem. - Eur. J.* **2006**, *12*, 6963−6975.

(37) Knappenberger, K. L.; Clayborne, P. A.; Reveles, J. U.; Sobhy, M. A.; Jones, C. E.; Gupta, U. U.; Khanna, S. N.; Iordanov, I.; Sofo, J.; Castleman, A. W., Jr. Anion Photoelectron Spectroscopy and Denstiy Functional Investigation of Diniobium-Carbon Clusters. *ACS Nano* **2007**, *1*, 319−326.

(38) Patzer, A. B. C.; Chang, C.; Sülzle, D. A Density Study of Small Ti_xC_y (x, y = 1−4) Molecules and Their Thermochemical Properties. *Chem. Phys. Lett.* **2014**, *612*, 39−44.

(39) Yeh, C. S.; Byun, Y. G.; Afzaal, S.; Kan, S. Z.; Lee, S.; Freiser, B. S.; Hay, P. Experimental and Theoretical Studies on $Nb_4C_4^{0/+}$: Reactivity and Structure of the Smallest Cubic Niobium-Carbon Cluster. J. *J. Am. Chem. Soc.* **1995**, *117*, 4042−4048.

(40) Pilgrim, J. S.; Brock, L. R.; Duncan, M. A. Photodissociation of Niobium-Carbon Clusters and Nanocrystals. *J. Phys. Chem.* **1995**, *99*, 544−550.

(41) Scheer, M.; Bilodeau, R. C.; Brodie, C. A.; Haugen, H. K. Systematic Study of the Stable States of C^-, Si^-, Ge^-, and Sn^- via Infrared-Laser Spectroscopy. *Phys. Rev. A: At., Mol., Opt. Phys.* **1998**, *58*, 2844−2856.

(42) Hotop, H.; Lineberger, W. C. Binding Energies in Atomic Negative Ions: II. *J. Phys. Chem. Ref. Data* **1985**, *14*, 731−750.

(43) Dean, J. A. Propertities of Atoms, Radicals, and Bonds. In *Lange's Handbook of Chemistry*, 15th ed.; McGraw-Hill., 1999; Section 4, pp 42 and 52.

(44) Arnold, D. W.; Bradforth, S. E.; Kitsopoulos, T. N.; Neumark, D. M. Vibrationally Resolved Spectra of C_1-C_{11} by Anion Photoelectron Spectroscopy. *J. Chem. Phys.* **1991**, *95*, 8753−8764.

(45) Duncan, M. A.; Knight, A. M.; Negishi, Y.; Nagao, S.; Judai, K.; Nakajima, A.; Kaya, K. Photoelectron Spectroscopy of $V_x(\mathrm{Coronene})_y$ Anions. *J. Phys. Chem. A* **2001**, *105*, 10093−10097.

(46) Wu, H.; Desai, S. R.; Wang, L.-S. Evolution of the Electronic Structure of Small Vanadium Clusters from Molecular to Bulklike. *Phys. Rev. Lett.* **1996**, *77*, 2436−2439.

(47) Zhao, T.; Zhang, S.; Guo, Y.; Wang, Q. TiC_2: A New Two-dimensinal Sheet Beyond MXenes. *Nanoscale* **2016**, *8*, 233−242.

(48) von Helden, G.; van Heijnsbergen, D.; Meijer, G. Resonant Ionization Using IR Light: A New Tool to Study the Spectroscopy and Dynamics of Gas-phase Molecules and Clusters. *J. Phys. Chem. A* **2003**, *107*, 1671−1688.

DOI: 10.1021/acs.jpca.6b00241
J. Phys. Chem. A 2016, 120, 1520−1528